LAUTECH Journal of Engineering and Technology 18 (2) 2024: 101-109
10.36108/laujet/4202.81.0290

Synthesis and characterisation of CaO nanoparticle from oyster shell using sol-gel method

[1]*Akatobi K. N., [1]Okolo B. I., [1]Adeyi O., [1]Oke E. O., [1]Dzarma G. W., [1]Nwosu-Obieogu K., [2]Ubani, L. O. C.

[1]*Department of Chemical Engineering, Michael Okpara University of Agriculture, Umudike. Nigeria.*
[2]*Department of Chemistry, Michael Okpara University of Agriculture, Umudike. Nigeria.*

Article Info

Article history:

Received: May 5, 2024
Revised: June 7, 2024
Accepted: June 10, 2024

Keywords:

CaO nanoparticles,
Characterisation,
Oyster shell,
Sol-gel.

Corresponding Author:
noble.kelechi@yahoo.com,
Tel.:+2348033352283

ABSTRACT

This study is aimed at the synthesis and characterization of CaO Nanoparticles from oyster shells. The sol-gel method was used to synthesize the particles, characterized using Fourier Transform Infrared Spectroscopy (FTIR), X-ray Diffraction (XRD) and Scanning Electron Microscopy/ Dispersive X-ray (SEM-EDX), Thermogravimetric/ Differential Thermal Analysis (TGA-DTA) and Brunaue-Emmett-Teller (BET) respectively. From the analysis conducted, the developed CaO nanoparticle has a point of zero charge of 5.6, indicating a stable charge balance. The particle was chemically characterized by the presence of some number of functional groups, most notably the –OH and C-H. The CaO nanoparticle was found to be crystalline in nature as revealed by XRD analysis. Findings from the BET indicated the material has a surface area of 344.528m^2/g, a specific pore volume of 0.170 cc/g and a pore diameter of 2.118 nm, indicating that it is mesoporous structurally. The results of the characterization reveal that the CaO nanoparticles present a suitable option for the treatment of wastewater based on the associated attributes.

INTRODUCTION

Nanotechnology has experienced significant growth over the last few decades as a relatively new field of study. Nanomaterial-based technology is inherently interdisciplinary, drawing from various scientific fields, including physics, chemistry, biology, and engineering. These disciplines utilize and benefit from the unique properties of nanomaterials to advance both theoretical research and practical applications (Deng *et al*., 2021). Scientists are becoming more interested in the manufacture of metallic nanoparticles from bio-oriented sources as a result of their availability and inexpensive processing (Thangamani and Bhuvaneshwari, 2019). Nanoparticles (NPs) made from plant and Animal resources are very important due to their numerous applications (Dauthal and Mukhopadhyay, 2016). Nanoparticles exhibit special properties due to the number of particles, improved surface area and surface interaction (Lakshmanan, 2013).

One major barrier to creating a sustainable future is the increasing amount of solid waste generation. Environmental and public health problems are caused by inadequate waste management techniques (Lulit *et al*., 2019). Oyster shell (OS) piles up along the coastal areas and result in many environmental issues including damage to landscape, health and sanitation problems, increase in pollution of marine eco-system due to illegal landfills, increased bad smell resulting from the decay of fresh remnants attached to oysters (Thrivene *et al*., 2017). Oyster is an important and commercially farmed marine animal with high market value (Cheng *et al*., 2021;

Hao, *et al*., 2021). Oyster cultivation has been in existence for over 2,000 years (Campbell and Hall, 2018). According to the Food and Agriculture Organization (FAO, 2018), global oyster production is estimated to be within 6.1 million tons per year, with an export increase of about threefold from 1997 to 2017. Oysters are highly nutritious and possess medicinal value, high in protein, active polysaccharides, taurine, vitamin, and mineral contents, with low fats, and an important shellfish, known for their delicious meat and calcareous shell (Guo, *et al*., 2020). OS consist mainly of calcium carbonate ($CaCO_3$; ~95%) in addition to a small proportion of organic matrix proteins (~0.1–5%), that form the skeleton/shell proteins. It is also composed of CaO, MgO, and some trace compounds (Upadhyay, *et al*., 2016). As an alkaline earth metal oxide, calcium oxide has a wide range of uses, including that of a catalyst (Banković-Ilić *et al*., 2017; Bharti *et al.,* 2019), an additive in refractory (Colombo *et al*., 2017), a removal agent for hazardous waste (Arul *et al*., 2018), an infused material to alter electrical and optical (dielectric) properties, an essential component for CO_2 capture, flue gas desulfurization, and the control of pollutant emissions (Khine *et al*., 2022).

Metal oxide nanoparticles have numerous applications, including catalytic processes, detectors, optoelectronic components, and remediation of the environment (Mirghiasi *et al*., 2014). Synthesis of calcium oxide nanoparticles depends on two main methods, bottom-up and top-down processes, with bottom-up being the most modern. These methods can further be classified into physical, chemical and biological methods (El-Sayed, 2020). The chemical method produces large quantities of nanoparticles, but requires capping agents for particle size stabilization, using chemicals with harmful environmental byproducts. The sol-gel method which is simple, inexpensive, efficient, sustainable, eco-friendly, and time-saving, requires no specialized equipment, no special skill, low temperature and no pressure, seems to address most of these drawbacks (Lulit *et al*., 2019). Hence the use of a sol-gel method for the synthesis of CaO nanoparticles from oyster shells might be used in wastewater treatment and other applications.

MATERIALS AND METHOD.

Materials

Oyster Shells (OS) were collected from Borokiri Waterside Port Harcourt, River State, Nigeria. The reagents necessary for the experimental procedures, include Hydrochloric acid (HCl- 35%–37% concentration), Sodium hydroxide (NaOH- 97% purity), Double distilled water, and Potassium Nitrate (KNO_3) were obtained from a certified dealer of laboratory chemicals in Aba, Abia State, Nigeria.

Method

Preparation of OS

The collected OS was shaken manually in an open basin to get rid of attached sand particles and debris. The OS was further soaked in warm water for 5 minutes, a process that was followed by thorough washing and rinsing in the double distilled water. The cleaned OS was sun-dried for 12 hours before the sample was oven-dried at 90^oC to eliminate absorbed moisture. The dried OS was ground into powder form and sieved using a 100µm screen. The resulting sample was packed in an air-tight pack to avoid absorption of moisture or caking.

Synthesis of calcium oxide nanoparticles (CaON)

Synthesis of the metal oxide nanoparticles through the sol-gel method was achieved through the adoption of methods used by (Lulit, *et al.,* 2019). The procedure involves the following four steps: preparation of a homogeneous solution, the formation of ‘sol’ by hydrolysis, the formation of ‘gel’ by condensation and drying, and calcination of the formed gel to produce CaON.

Point of zero charge (pHZPC)

The point of zero charge is regarded as the pH at which the charge on the CaON surface is zero (pH_0). It is an important property that determines the surface electrical neutrality of the particle (Okolo *et al.*, 2020). The point of zero charge (pH_{ZPC}), of the CaON was determined using the salt addition method (Mahmood, *et al.*, 2011). In this method, 0.01M KNO_3 solution was prepared and the pH was adjusted from 2 to 10 ($pH_{initial}$) using 0.1M HCl and 0.1M NaOH. Carefully, 0.6g of CaON was added to 100 ml of each of the adjusted pH solutions in a conical flask. This was agitated with a magnetic shaker for 48 hours at room temperature. The pH_{final} value of the supernatant was measured. A graph of change in pH (pH_{final}- $pH_{initial}$) was plotted against $pH_{initial}$. The pH at which the curve cuts pH_0 was used as the pH_{zpc} (Okolo, *et al.*, 2020).

Characterization of CaON

CaON was characterized using Fourier transform infrared (FTIR), X-ray diffraction study (XRD), Scanning electron microscopy (SEM-EDX), Thermal analysis (TGA- DTA), Brunaue-emmett-teller (BET) surface area analysis.

DISCUSSION OF RESULTS

Point of zero charge (pH_{ZPC})

The pH_{ZPC} reveals information about the efficiency, potentials, dynamics and available binding sites on the surface of the particles (Ranote, *et al.*, 2019; Okolo, *et al.*, 2020). To understand the efficiency and dynamics, it is important to determine the point of zero charge. The point at which the curve cuts the x-axis is defined as pH_{ZPC} (Abderrak *et al.*, 2023). From the plot presented in Figure 1, the pH_{ZPC} value of the CaON particles in this work was 5.6. The pH_{pzc} of the particle under investigation was less than 7, indicating that the stabilized ions in an aqueous solution have perfect charge balance in the acidic region.

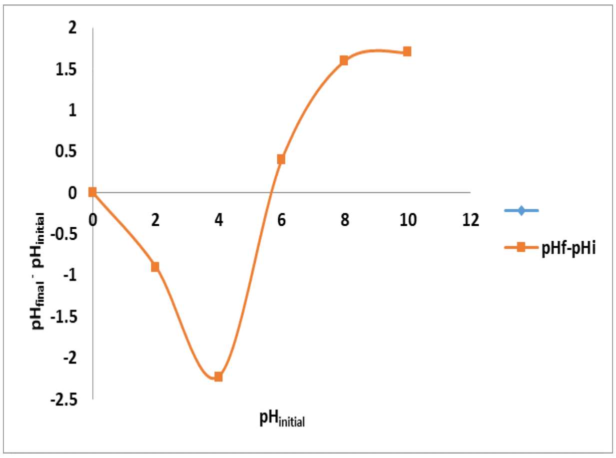

Figure 1: Point of zero charge (pHZPC) for CaON

Fourier Transform Spectroscopy (FTIR)

The Fourier transform infrared spectroscopy (FTIR) was used to investigate the important functional groups in CaON. The Spectrum representing the various functional groups in the developed particle is presented in Figure 2.

The broad band at the region 3652.8 – 3205.5cm^{-1} is attributed to –OH stretching of a polymeric compound. The band at 2922.2 cm^{-1}, is a result of asymmetric vibration of C-H which represents the aliphatic nature of the particles. The peak at 2344.5 cm^{-1} indicated alkane –C-H stretching vibration or –OH stretch of carboxyl acids (Coskun *et al.*, 2018; Yahya, *et al.*, 2020c). The peak at 2322.1cm^{-1} shows the presence of alkane –C-H stretching vibration or –OH stretch of carboxyl acids (Joshi and Pokharel, 2014). The band present at 2109.7cm^{-1} to 1893.5 indicates the presence of a C=O group. The peak at 1581.8cm^{-1} is assigned to C=O stretching (amide I) and NH stretching (amide II), and the peak observed at 1420.54 cm^{-1}and 1162.9 cm^{-1} were attributed to symmetric and asymmetric stretching vibration in alkane, alkenes and alkynes (Hajji *et al.*, 2017). The out plane bending –OH vibration are observed at 745.5cm^{-1} (Wang *et al.*, 2016a; Dil *et al.*, 2017).

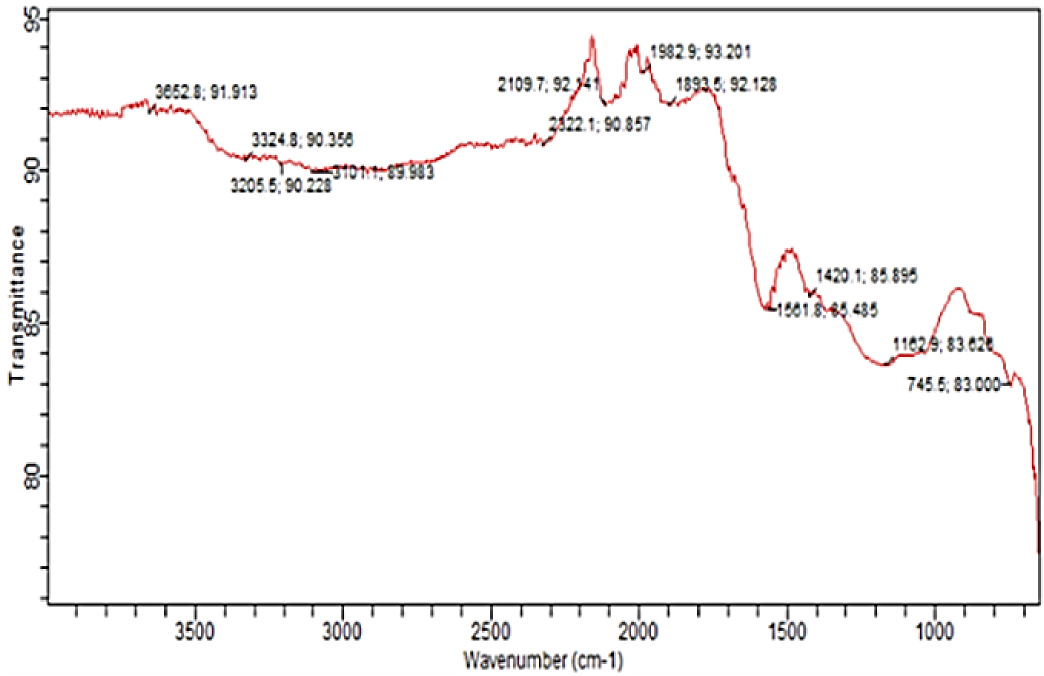

Figure 2: FTIR of CaON

X-ray diffraction (XRD).

XRD patterns have long been used to describe key features of a chemical, like the kinds and composition of its crystalline phases. The XRD study included the theta-2 values of the different peaks in Figure 3. Comparing the X-ray diffraction pattern, the CaON exhibit a very sharp peak at 2θ = 26.5^oC and a sharp crystalline peak at 2θ = 13.5^oC where a reduced intensity of the peak at 2θ = 30.5^oC and the disappearance of peak at 2θ = 48.5^oC are observed, indicating the loss of crystallinity due to cross-linking (Rubangakene *et al.*, 2023).

Scanning electronic microscopic and Energy disperse x-ray (SEM-EDX).

The examination of the CaON surface morphology was conducted using SEM. The microscopic image of the particle as presented in Figure 4 indicated a non-uniformly organized pore sizes and shape, providing strong reactive sites. The structure of the material can be attributed to the incorporation of the metallic oxide (CaO) into the carbonized OS. This is similar to findings reported by Mohammed, Ibrahim and Zulkifli (2021) in their study synthesis of nano-adsorbent from fruit shells. Another study by Herrera-barros and Tejada-Tovar (2022) reported similar results of nanoparticle development from residual biomass using green synthesis.

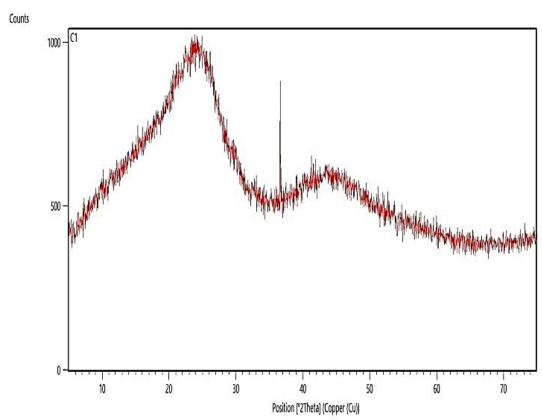

Figure 3: XRD of CaON

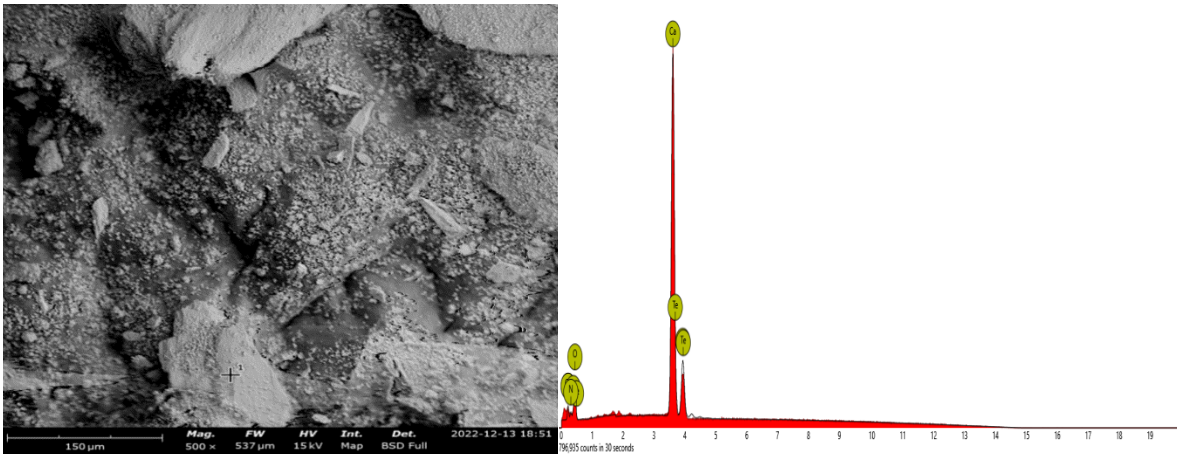

Figure 4: SEM and EDX of CaON

Table 1: EDX of CaON

Element Number	Element Symbol	Element Name	Atomic Conc.	Weight Conc.
8	O	Oxygen	52.30	30.65
20	Ca	Calcium	35.88	52.67
7	N	Nitrogen	9.27	4.76
52	Te	Tellurium	2.55	11.92

Lulit *et al.* (2019) synthesis of Nano-Calcium Oxide from Waste Eggshell by Sol-Gel Method, showed that the nanoparticles are approximately spherical in morphology agglomerating to each other and showed the polycrystalline character of the nanoparticle.The size of the calcium oxide nanoparticle was reduced after drying, followed by calcination of the $Ca(OH)_2$ gel to release CO_2 and H_2O. The corresponding EDX spectrum in Table 1, indicated the presence of only four major constituents O, Ca, N and Te. Similar types of pore arrangement were observed by Ranote *et al.(*2019).

Thermogravimetric analysis (TGA) and differential thermal analysis (DTA).

The thermogravimetric and differential thermal analysis were used to determine the thermal stability of the CaON. The DTA curve showed the mid-point decomposition temperature as presented in Figure 5. It is observed from the thermogram that the CaON has stage-wise weight loss in the following three steps: (1) within the temperature range of $30^oC - 250^oC$ was due to the loss of physically adsorbed water (2) $250^oC - 500^oC$ was attributed mainly to the loss of lattice water and NH_2 group. (3) At higher temperature (500^oC-700^oC) might be due to structural deformation. The analysis of DTA curve of the material revealed that the process is endothermic up to a temperature of 400^oC may be due to the loss of external water and other major endothermic peaks which corresponds to a loss of –CO, NH_2 functional groups (Wu, *et al*., 2015).

Brunauer-Emmett-Teller (BET) analysis

BET analysis was performed to assess the surface area and pore sizes of the developed CaON. The characteristic surface area, pore diameter and pore volume attributed to the development of CaON are presented in Table 2. From the Table, it can be observed that the CaON has a high specific surface area (344.528m^2/g) providing enough active sites for reactions. The average pore diameter of the CaON was found to be 2.118nm, indicating that the material under consideration is structurally mesoporous because the pore diameters were larger than 2nm but smaller than 50 nm (Srivastava, 2021, Uko, *et al.*, 2022, Ehsan, Naser and Ershad, 2024). The CaON was also reported to have a pore volume of 0.170cc/g, revealing a good potential, which can be directly related to the high pore volume (Ehsan, Naser and Ershad, 2024).

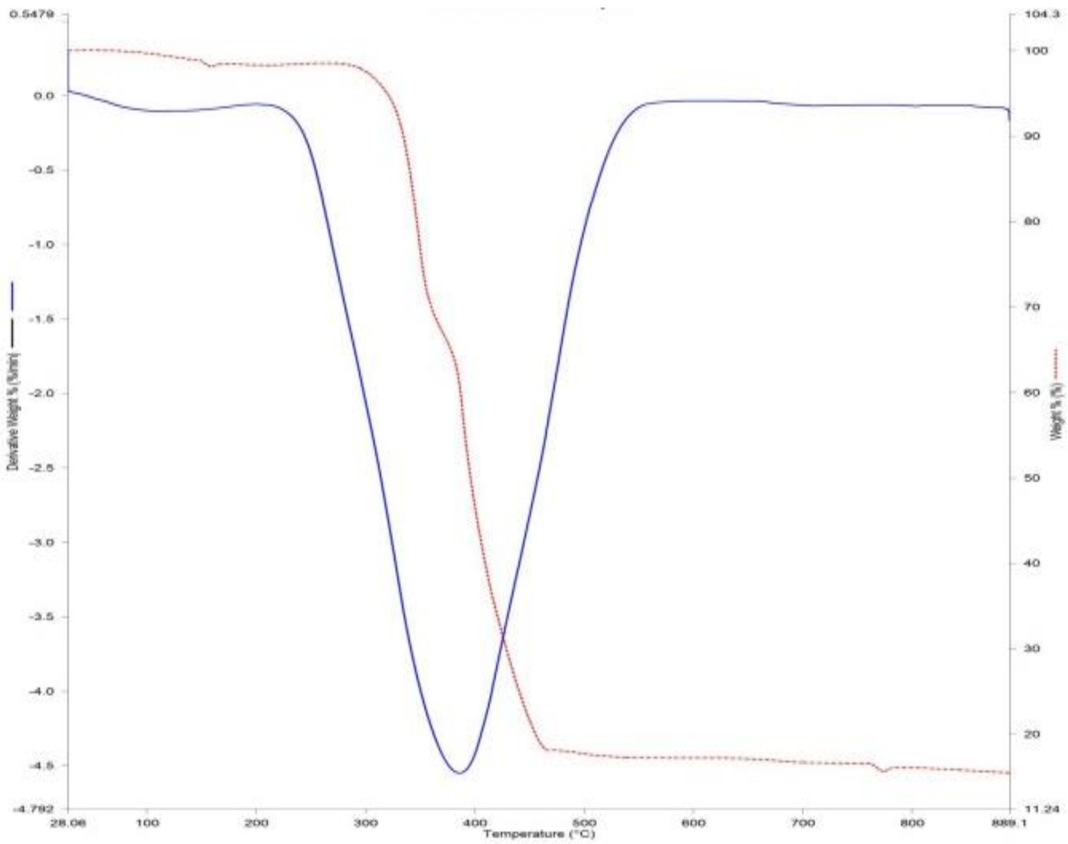

Figure 5: Thermogravimetric analysis (TGA) and differential thermal analysis (DTA) of CaON

Table 2: BET of CaON

Parameters	CaO nanoadsorbent
Surface area (m^2/g)	344.528
Pore volume (cc/g)	0.170
Pore Diameter (nm)	2.118

CONCLUSIONS

This study was aimed at providing a more efficient, cost-effective, sustainable and eco-friendly nanoparticle that can be used in wastewater treatment options through the development and characterization of CaON from OS. The study adopted the sol-gel method to synthesise the nanoparticle from the selected biomass, and the developed product was characterized using some approaches. Findings from the study reveal that the point of zero charge of the adsorbent was 5.6, indicating a good charge balance. The developed CaON was also discovered to have a crystalline arrangement with a heterogeneously arranged pore as revealed from the surface characterization. Additionally, the material was found to have sufficient surface area and pore volume, while having adequate pore sizing to permit adsorption. From the findings, it can be concluded the developed CaON presents good potential for usage in synthetic wastewater treatment.

REFERENCES

Abderrazak, H., Djamal, A., Abdelkrim R., Abdallah R., Ammar, Z., Mohammad, M., Bachir B. S., Pawel P & Jesus S. G (2023). Investigation of adsorption kinetics and isothermal thermodynamics for optimizing methylene blue adsorption onto a modified clay with cellulose using the response surface approach. Biomass Conversion and

Biorefinery https://doi.org/lO.1007/sI 3399-023- 04397-I.

Arul, E., Raja, K., Krishnan, S., Sivaji, K., & Das, S. J. (2018). Bio-Directed Synthesis of Calcium Oxide (CaO) Nanoparticles Extracted from Limestone Using Honey. Journal of Nanoscience and Nanotechnology, 18(8), 5790–5793. https://doi.org/10.1166/jnn.2018.15386

Banković-Ilić, I. B., Miladinović, M. R., Stamenković, O. S., & Veljković, V. B. (2017). Application of nano CaO–based catalysts in biodiesel synthesis. Renewable and Sustainable Energy Reviews, 72, 746–760. https://doi.org/10.1016/j.rser.2017.01.076

Bharti, P., Singh, B., & Dey, R. K. (2019). Process optimization of biodiesel production catalyzed by CaO nanocatalyst using response surface methodology. Journal of Nanostructure in Chemistry, 9(4), 269–280. https://doi.org/10.1007/s40097-019-00317-w

Campbell, M. D. & Hall, S. G. (2018). Hydrodynamic Effects on Oyster Aquaculture Systems: a Review. Rev. Aquacult 11, 896–906. doi:10.1111/raq.12271.

Cheng, S., Tu, M., Liu, H., An, Y., Du, M. & Zhu, B. (2021). A Novel Heptapeptide Derived from Crassostrea gigas Shows Anticoagulant Activityby Targeting for Thrombin Active Domain. Food Chem. 334, 127507. doi:10.1016/j.foodchem.2020.127507.

Colombo, K., Ender, L., & Barros, A. A. C. (2017). The study of biodiesel production using CaO as a heterogeneous catalytic reaction. Egyptian Journal of Petroleum, 26(2), 341–349. https://doi.org/10.1016/j.ejpe.2016.05.006

Coskun, R., Savci, S & Delibas, A. (2018). Adsorption properties of activated almond shells for methylene blue (MB). Environmental Research & Technology, Vol. 1 (2), 2018. http ://dergipark. gov.tr/ert.

Dauthal, P., & Mukhopadhyay, M. (2016). Supporting Information for Publication Noble Metal Nanoparticles: Plant Mediated Synthesis, Mechanistic Aspects of Synthesis 2 and Applications. 55, 9557–9577.

Deng, Z., Gong, M., & Li, Y. (2021). Synthesis of Different Nanoparticles for Biological Application. Journal of Physics: Conference Series, 2133(1). https://doi.org/10.1088/1742-6596/2133/1/012004

Dil. E.A., Ghaedi, M & Asfaram, A (2017). The performance of nanorods material as adsorbent for removal of azo dyes and heavy metal ions: application of ultrasound wave, optimization and modeling. Ultrason Sonochem 34:792-8

Ehsan, A., Naser, S. & Ershad, S. (2024) 'Optimization of Removal of Ibuprofen Antibiotic from Water in the Presence of ZnO/Fe203 and ZnO/activated Carbon Nanoparticles. Using Response Surface Methodology.

El-sayed, M.E.A (2020). Nanoadsorbents for water and water remediation, *Science of Total Environment* (2020), https://doi.org/10.1016/j.scitotenv.2020.139903.

FAO, (2018). Available at: https://www.fao.org/fishery/en/statistics/en.

Guo, Z., Zhao, F., Chen, H., Tu, M., Tao, S. & Wang, Z. (2020). Heat Treatments of Peptides from Oyster (Crassostrea gigas) and the Impact onTheir Digestibility and Angiotensin

I Converting Enzyme Inhibitory Activity. Food Sci. Biotechnol. 29 (7), 961–967.

Hajji, S, Slama, R.B., Salem, B., Hamdi, M., Jellouli, K.., Ayadi, W., Nasri, M & Boufi. S (2017). Nanocomposite films based on chitosan-poly(vinylalcohol) and silver nanoparticles with high antibacterial and antioxidant activities. *Process Saf Environ Prot* 111:112-121. https://doi.org/10.101 6/j .psep.2017.06.018.

Hao, L., Wang, X., Cao, Y., Xu, J., & Xue, C. (2021). A Comprehensive Review of Oyster Peptides: Preparation, Characterisation and Bioactivities. Rev. Aquacult14, 120–138.

Herrera-Barros, A., Candelaria, T.T & Ángel D. G. D (2022). 'Green Nanoparticle-Aided Biosorption of Nickel Ions Using Four Dry Residual Biomasses : A Comparative Study'. *Sustainability* 2022, *14*(12), 7250; https://doi.org/10.3390/su14127250.

Joshi, S. & Pokharel, B. P. (2014). Preparation and Characterization of Activated Carbon from Lapsi (*Choerospondias axillaris*) Seed Stone by Chemical Activation with Potassium Hydroxide. Journal of the Institute of Engineering, Vol. 9, No. 1, pp. 79-88 .https://doi.org/10.31 26/jie.V9i I .w673.

Khine, E. E., Koncz-Horvath, D., Kristaly, F., Ferenczi, T., Karacs, G., Baumli, P., & Kaptay, G. (2022). Synthesis and characterization of calcium oxide nanoparticles for CO2 capture. Journal of Nanoparticle Research, 24(7). https://doi.org/10.1007/s11051-022-05518-z

Lakshmanan, R (2013). Application of magnetic Nanoparticles and reactive filter materials for wastewater treatment (Doctoral dissertation). Royal Institute of Technology, School of Biotechnology, Stockholm.

Lulit H., Natnael S., Dure M., Thriveni, T., Ramakrishna, C & Ji, W. A (2019). Synthesis of Nano-Calcium Oxide from Waste Eggshell by Sol-Gel Method Sustainability,11(11), 3196; https://doi.org/10.3390/sul 11 13196.

Mahmood, T., Saddique, M. T., Naeem, A., Westerhoff, P., Mustafa, S. & Alum, A. (2011). Comparison of different methods for the point of zero charge determination of NiO. Ind Eng Chem Res 50:10017–11003

Mirghiasi, Z., Bakhtiari, F., Darezereshki, E., & Esmaeilzadeh, E. (2014). Preparation and characterization of CaO nanoparticles from Ca(OH)2 by direct thermal decomposition method. Journal of Industrial and Engineering Chemistry, 20(1), 113–117. https://doi.org/10.1016/j.jiec.2013.04.018

Mohammed, A. J., Ibrahim, M. H., Zulkifli, S. Z. & Salman, M. J. (2021). 'Synthesis and Characterization of a Nano Adsorbent Derivative Derived from Grape Seeds for Cadmium Ion Removal in an Aqueous Solution'. *Water* 2021, *13*(20),2896; https://doi.org/10.3390/w13202896

Okolo, B.I.; Oke E.I.; Agu Chinedu M.; Adeyi O.; Nwosu-Obieogu K. & Akatobi K.N. (2020). Adsorption of lead (lI) from aqueous solution using Africa elemi seed, mucuna shell and oyster shell as adsorbents and optimization using Box-Behnken design. Applied Water Science (2020) 10:201 https://doi.org/10.1007/s 1320 l-020-01242-y.

Ranote, S.; Kumar, D.; Kumari, S.; Kurnar, R.; Chauhan, G. S. & Joshi, V. (2019). Green synthesis of Moringa oleifera gum-based bifunctional polyurethane foam braced with ash for rapid and efficient dye removal. Chemical Engineering 361, 1586-1596.

Rubangakene, N O., Marwa E., Ahmed E., Manabu F., Sekiguchi, H., & Hassan S. (2023). 'Novel nanobiosorbent materials from thermal catalytic degradation of green pea waste for cationic and anionic dye decolorization', *Biomass Conversion and Biorefinery.* 13(16), pp. 14873-14888. Available at: https://doi.org/1 0.1007/s 1339 9-022-03299-y.

Srivastava, V. (2021). 'Green route synthesis of metal based nanoparticles and their composites with polymers for industrial applications'.

Thangamani, N., & Bhuvaneshwari, N. (2019). Green synthesis of gold nanoparticles using Simarouba glauca leaf extract and their biological activity of micro-organism. Chemical Physics Letters, 732. https://doi.org/10.1016/j.cplett.2019.07.015

Thriveni T., Chilakala, R & Ji W. A (2017). Environmental Effect of the Coffee Waste and Anti-Microbial Property of Oyster Shell Waste Treatment. Journal of Energy Engineering, Vol. 26, No. 2, pp.39~49(2017).

Uko, C. A., Tijani, J. O., Abdulkareem, A. S., Mustapha, S., Egbosiuba, T. C & Muzenda, E (2022). 'Adsorptive properties of MgO/W03 nanoadsorbent for selected heavy metals removal from indigenous dyeing wastewater', *Process Safety and Environmental Protection,* 162, pp. 775-794. Available at: https://doi .org/ 10.101 6/j .psep.2022.04.057.

Upadhyay, A. K., Bankoti, N. S. & Rai, U. N. (2016). Studies on sustainability of simulated constructed wetland system for treatment of urban waste, Design and operation. J. Environ. Manag. 169, 285e292.

Wang, C., Alpatova, A., McPhedran, K. N. & Gamal, E. M. (2016a). Coagulation/flocculation process with polyaluminum chloride for the remediation of oil sands process- affected water: Performance and mechanism study. Journal of Environmental Management 160, 254-262.

Wu, W., Yang, L., Chen, S., Shao, Y., Jing, L., Zhao, G., & Wei, H. (2015). Core-Shell nanospherical polyprrole/graphene Oxide Composites for high performance Supercapacitors. RSC Adv. 2015, 5, 91645-91653.

Yahya, M. D., Obayomi, K. S., Abdulkadir, M. B., Iyaka Y. A. & Olugbenga A. G. (2020). Characterization of cobalt ferrite-supported activated carbon for removal of chromium and lead ions from tannery wastewater via adsorption equilibrium. Water Science and Engineering 2020, 13(3): 202e213 https://doi.org/ 10.1016/j.wse.2020.09.007 1674-2370.